JOURNAL OF MATERIALS SCIENCE 28 (1993) 5040–5044

Electrical resistivity and Hall effect of K–$FeCl_3$ graphite intercalation compounds

O. EL-SHAZLY*, S. G. TAWFIK, A. K. IBRAHIM, I. H. IBRAHIM, E. F. EL-WAHIDY
Department of Physics, Faculty of Science, Alexandria University, Alexandria, Egypt

Both in-plane as well as *c*-axis electrical resistivity of Stage 2 and Stage 5 K–$FeCl_3$ graphite intercalation compounds were measured from room temperature down to 12 K by using a standard four-probe method. The in-plane electrical resistivity exhibited a metallic behaviour. The *c*-axis resistivity exhibited an activated behaviour and the data were fitted to a model which assumes a variable-range hopping conduction in parallel with band conduction. The Hall effect was measured in a low magnetic field up to 5 kG at temperatures 300, 77 and 12 K. The Hall coefficient was found to be positive, indicating that the conduction takes place by holes. The carrier concentrations were calculated using a one-carrier model.

1. Introduction

Graphite has a relatively poor conductivity due to the low density of electrons and holes. The conductivity of graphite could be greatly modified by the insertion of atomic or molecular layers of intercalant between the graphite layers [1]. The charge transfer between intercalant and graphite layers results in an increased density of highly mobile carriers. Therefore, the electrical conductivity of graphite intercalation compounds (GICs) are enhanced. Most of the research in the field of GICs has been devoted, so far, to the binary graphite intercalation compounds (BGICs) [1, 2].

Ternary graphite intercalation compounds (TGICs) result from intercalating two distinct intercalant species in the host graphite galleries. Most of the TGICs, which have been reported so far, are either donor–donor type, such as K–Cs TGICs [3] or acceptor–acceptor type, such as $BiCl_3$–$ReCl_4$ TGICs [4], $CoCl_2$–$FeCl_3$ TGICs [5] or $TlCl_3$–$TlBr_3$ TGICs [6]. Interest in TGICs was recently stimulated by realizing that they offer exciting new opportunities for the study of physical phenomena in low dimensions as well as for practical applications.

Several authors reported their results on donor–acceptor TGICs. Suzuki *et al.* [7] succeeded in preparing $CoCl_3$–K TGIC. This compound was synthesized by sequential intercalation of potassium atoms into $CoCl_2$ BGIC. A new family of TGICs formulated as M–Bi TGIC (M = K, Rb, Cs) have been synthesized by Lagrange *et al.* [8]. They measured the electrical resistivity, both parallel, ρ_a, and perpendicular, ρ_c, to the basal plane in the temperature range from 1.4–295 K. The in-plane behaviour was found to be metallic in all cases, while the *c*-axis resistivity showed a thermally activated behaviour, except for the richest compounds. Pernot *et al.* [9] examined ρ_a and ρ_c for Stages 1 and 2 of $AlCl_3$–$CoCl_2$ and $AlCl_3$–$CuCl_2$ TGICs. Both ρ_a and ρ_c showed a metallic behaviour with temperature. Guérard *et al.* [10] obtained ternary compounds by direct reaction on graphite of the alkali metal hydrides MH (M = Na, K, Rb, Cs). Guérard *et al.* [10] found that the in-plane conductivity was comparable to that of the binary compounds with the alkali metals. Measurements in the *c*-axis direction indicated that ρ_c increases with temperature for Stage 1, whereas, for Stage 5 with sodium hydride, the behaviour is reversed, as usually appears with binary or ternary GICs.

The synthesis of potassium and $FeCl_3$ into graphite provides a unique way of obtaining a novel TGIC with a combination of different kinds of intercalants such as alkali metals, which gives a donor type, and transition metal chlorides, which gives an acceptor type. We are interested in studying the electrical properties of K–$FeCl_3$ TGIC, namely the electrical resistivity and the Hall effect.

2. Experimental procedure

The ternary graphite intercalation compound was prepared from a successive intercalation process using a highly oriented pyrolytic graphite (HOPG). The starting material (Stages 2 and 5 $FeCl_3$ GICs) was prepared from HOPG by using the standard two-temperature zone method. Potassium was intercalated into $FeCl_3$ GIC by the same method. Details of the intercalation process were given elsewhere [11].

The in-plane and along the *c*-axis electrical resistivity of HOPG and Stages 2 and 5 K–$FeCl_3$ TGICs were measured using the standard four-probe method. Thin samples, typically of dimensions

* Author to whom all correspondence should be addressed.

0022–2461

$1.15 \times 0.25 \times 0.001$ cm^3, were used for the in-plane measurements, whereas thick samples, of dimensions $1.58 \times 0.47 \times 0.34$ cm^3, were used for the measurements along the c-axis. Thin copper wires were attached to the sample using silver paint. The temperature dependence of resistivity was measured between 300 and 12 K. A closed-cycle refrigeration system from Air Products was used for cooling the samples, and its temperature was measured by using a Kp–Au 0.07 at% Fe thermocouple.

The Hall voltage was measured for the in-plane samples for HOPG as well as TGICs in the low magnetic-field range (up to 5 kG) at temperatures 300, 77 and 12 K.

3. Results and discussion

3.1. In-plane resistivity

The temperature dependence of the in-plane resistivity normalized to room temperature value, $(\rho/\rho_{300\text{ K}})_a$, of HOPG is shown in Fig. 1. It is seen that the in-plane resistivity of HOPG exhibits a metallic behaviour, i.e. ρ_a increases with increasing temperature. This behaviour was also observed for single-crystal graphite, as measured by Kinchin [12] and Soule [13].

The temperature dependence of resistivity of HOPG indicates that there are two regions of interest; the first region extends from 300 K to about 80 K, while the other region starts below 80 K down to 12 K. It is interesting to notice that in each region, ρ_a exhibits a power-dependence on T, i.e.

$$\rho_a \propto T^{n_i} \qquad i = 1, 2 \tag{1}$$

It was found that the exponents n_1 and n_2 have the values 0.20 and 0.48, respectively. Similar behaviour for ρ_a was observed for Kish graphite [14], where it was found that n_1 and n_2 have the values 0.2 and 1.0 for Regions 1 and 2, respectively.

The temperature dependence of the resistivity ratio $(\rho/\rho_{300\text{ K}})_a$ of Stages 2 and 5 K–$FeCl_3$ TGICs is shown in Fig. 2. It is clear that the rate of decrease of resistivity of Stage 2 with decreasing temperature is faster than that of Stage 5. The in-plane resistivity of Stages 2 and 5 K–$FeCl_3$ TGICs shows a metallic temperature dependence, which is typical for all BGICs. This behaviour also seems to be characteristic for TGICs. For example, Marêché *et al.* [15] found that ρ_a of K–Bi TGIC exhibits a metallic behaviour and McRae *et al.* [16] obtained the same behaviour for Rb–Bi TGIC and Cs–Bi TGIC.

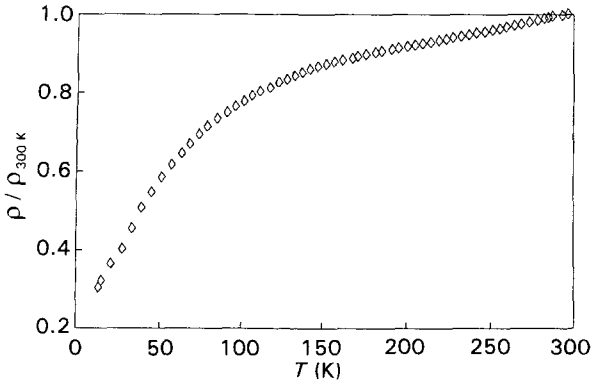

Figure 1 Temperature dependence of the in-plane resistivity ratio of HOPG.

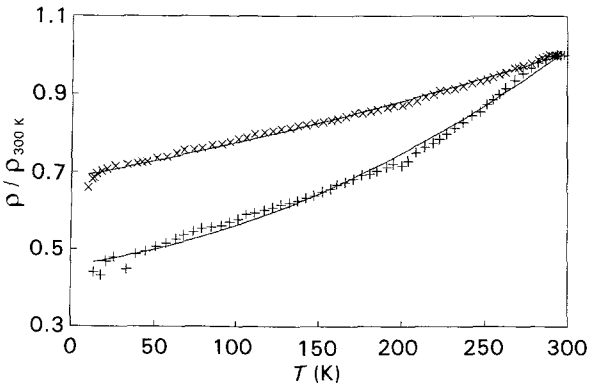

Figure 2 Temperature dependence of the in-plane resistivity ratio of Stages (+) 2 and (×) 5 K–$FeCl_3$ TGICs, experimental data and (——) fitting.

TABLE I In-plane fitting parameters of the equation $\rho(T) = A + BT + CT^2$ for Stages 2 and 5 K–$FeCl_3$ TGICs

	A	B (10^{-4} K^{-1})	C (10^{-6} K^{-2})
Stage 2	0.457	6.43	4.04
Stage 5	0.685	8.15	0.83

The quadratic equation

$$\rho(T) = A + BT + CT^2 \tag{2}$$

was used for fitting the experimental results of ρ_a for Stages 2 and 5 K–$FeCl_3$ TGICs and gave satisfactory results, as shown in Fig. 2. This temperature dependence of resistivity was mostly used for the interpretation of the BGICs for donors as well as acceptors [1]. The coefficients A, B and C, normalized to room-temperature resistivity values, are listed in Table I. In the high-temperature region, the resistivity is linear with temperature, which is consistent with an electron–phonon scattering mechanism. At lower temperatures, the change in the resistivity is quadratic with temperature, which describes a carrier–carrier scattering mechanism [1]. This effect has a large temperature range over which this term contributes significantly.

3.2. c-axis resistivity

The c-axis temperature dependence of resistivity ratio $(\rho/\rho_{300\text{ K}})_c$ of HOPG is shown in Fig. 3. It is clear that the resistivity increases monotonically with decreasing temperature from room temperature until about 40 K, then it starts to decrease with decreasing temperature. This behaviour indicates that the nature of conduction carriers at high temperatures differs from that at low temperatures. Above about 40 K, the temperature coefficient of resistivity ($d\rho/dT$) is negative, which indicates an activated conduction behaviour. Below about 40 K, $d\rho/dT$ is positive, indicating a metallic

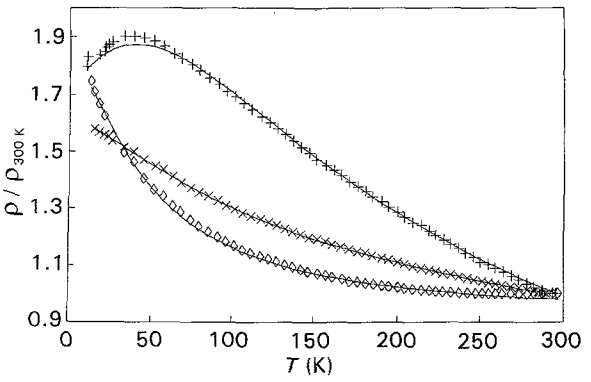

Figure 3 Temperature dependence of the resistivity ratio the c-axis of (+) HOPG, Stages (◇)2 and (×)5 K–$FeCl_3$ TGICs, experimental data and (——) fitting.

conduction behaviour. It was found that ρ_c for pyrolytic graphite [17] has a negative temperature coefficient of resistivity along the whole temperature range from room temperature down to about 10 K. Also, polycrystalline graphite samples of graphite [18] showed a similar behaviour.

The c-axis resistivity ratio $(\rho/\rho_{300\,K})_c$ as a function of temperature of Stages 2 and 5 K–$FeCl_3$ TGICs are shown in Fig. 3. It is clear that the temperature dependence of ρ_c of Stages 2 and 5 TGICs is different from that of HOPG. ρ_c for K–$FeCl_3$ TGICs increases with decreasing temperature from room temperature down to 12 K. For Stage 2, it can be noticed that ρ_c increases slowly from room temperature until about 110 K, below which the increase in ρ_c becomes much faster with decreasing temperature. For Stage 5, the rate of increasing of ρ_c with decreasing temperature is faster than that of Stage 2.

It is clear that the c-axis resistivity of TGICs has a negative temperature coefficient at all temperatures. This behaviour is different from that observed for most BGICs, where low-stage compounds have a c-axis resistivity which increases with increasing temperature, while for higher stages as well as for HOPG, the tendency is reversed. For example, the temperature dependence of c-axis resistivity of Stage 5 potassium BGIC shows an activated behaviour [19]. Powers *et al.* [20] studied the temperature dependence of c-axis resistivity for different stages of $FeCl_3$ BGICs. They found that stages less than 5 have a metallic behaviour, but with a very small slope. For higher stages, Powers *et al.* [20] obtained an activated conduction behaviour. On the other hand, Pernot *et al.* [9] found that ρ_c of Stages 1 and 2 for $CoCl_2$–$AlCl_3$ TGICs and $CuCl_2$–$AlCl_3$ TGICs has a metallic behaviour, which is similar to $AlCl_3$ BGIC.

A model for the c-axis resistivity, which was first used by Powers *et al.* [20] for $FeCl_3$ BGICs samples, was used to analyse the resistivity data of c-axis measurements of all samples. According to that model, it was assumed that two mechanisms are affecting the c-axis conduction; a band conduction (BC) which is in parallel with a variable range hopping (VRH) mechanism which is applicable to lightly doped semiconductors [21]. In the case of GICs, the intercalant plays the role of the impurity and the degree of compensation depends on the stage. The total resistivity can be expressed as

$$\rho = \frac{\rho_{VRH}\,\rho_{BC}}{\rho_{VRH} + \rho_{BC}} \tag{3}$$

where ρ_{VRH} is given by

$$\rho_{VRH} = \rho_0\left(\frac{T_0}{T}\right)^{n_1} e^{(T_0/T)^{n_2}} \tag{4}$$

where ρ_0 is a function of doping and compensation, T_0 is a function of density of states, n_1 and n_2 depend on the dimensionality of the system, and

$$T_0 = \frac{\beta}{g(\mu)a^3k_B} \tag{5}$$

where $g(\mu)$ is the density of states at the Fermi level, a is the localization radius, k_B is Boltzmann's constant and β is numerical coefficient. ρ_{BC} is given by

$$\rho_{BC} = \rho_m T^{n_3} + \rho_r \tag{6}$$

where ρ_m is a function of the concentration and the effective mass of the charge carriers, n_3 is the power of the temperature, and ρ_r is the residual resistivity due to static imperfections. It was indicated that band conduction dominates at temperatures below 120 K.

It was found that the c-axis model fits well to the experimental data, as shown in Fig. 3. The values of the fitting parameters of HOPG, Stages 2 and 5 K–$FeCl_3$ TGICs are listed in Table II. The same model was also applied by Sugihara *et al.* [22] to analyse the c-axis resistivity data of $Co_{1-x}Fe_xCl_2$ TGICs.

3.3. Hall voltage

The Hall voltage, V_H, of HOPG as a function of the magnetic field at temperatures 300, 77 and 12 K is shown in Fig. 4. It is clear that the magnitude of V_H increases with decreasing temperature. It is interesting to notice that at 77 K, V_H changes sign from negative to positive to negative once more. This can be attributed to the close balance of electron-hole concentrations and mobilities. On the other hand, it can be

TABLE II c-axis fitting parameters of the VRH in parallel with the BC equation for HOPG, Stages 2 and 5 K–$FeCl_3$ TGICs

	ρ_0	T_0	n_1	n_2	ρ_m ($\times 10^{-3}$)	n_3	ρ_r
HOPG	0.164	853.96	0.542	0.394	7.41	1.0	1.748
Stage 2	0.434	1012.67	−0.351	0.407	4.03	1.0	1.766
Stage 5	0.828	802.82	−0.049	0.439	−0.83	1.0	1.601

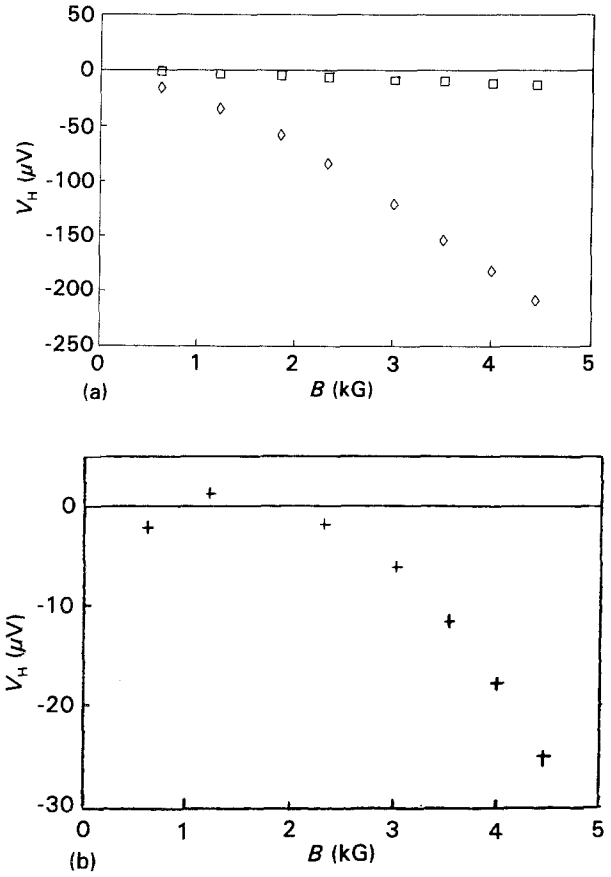

Figure 4 (a) Hall voltage of HOPG at temperatures (□) 300 and (◇) 12 K. (b) Hall voltage of HOPG at (+) 77 K.

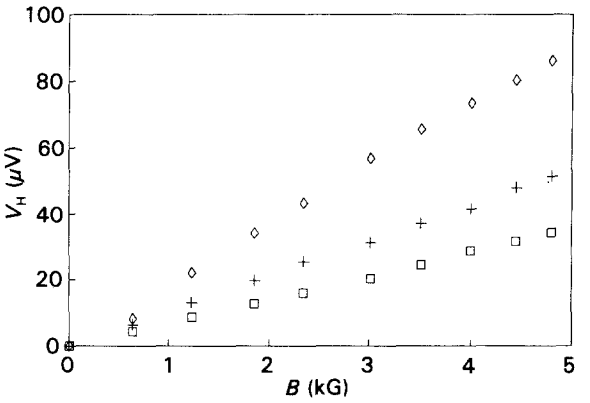

Figure 5 Hall voltage of Stage 2 K–$FeCl_3$ TGIC at temperatures (□) 300, (+) 77 and (◇) 12 K.

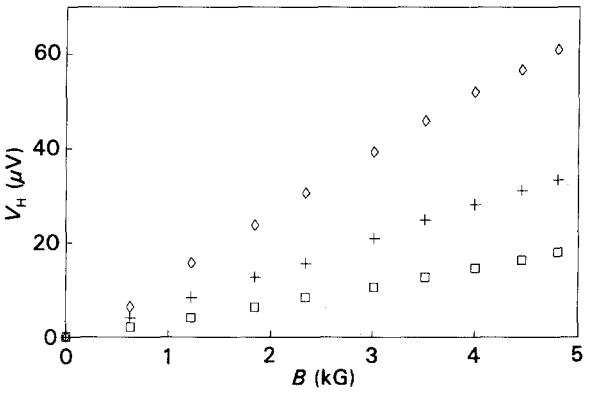

Figure 6 Hall voltage of Stage 5 K–$FeCl_3$ TGIC at temperatures (□) 300, (+) 77 and (◇) 12 K.

noticed that V_H has negative values at 300 and 12 K at all magnetic field values. This indicates that electrons are the majority charge carriers at those temperatures. Our measurements are in good agreement with that of Spain *et al.* [23]. Similar results were obtained by Tsuzuku *et al.* [24] for highly oriented graphites.

The field dependence of the Hall voltage, V_H, at 300, 77 and 12 K for Stages 2 and 5 K–$FeCl_3$ TGICs are shown in Figs 5 and 6, respectively. It is clear that V_H has a small value for TGICs and has a small change with temperature, which is a typical metallic behaviour. Dresselhaus and Dresselhaus [1] indicated that the magnitude of the Hall coefficient in the intercalation compounds tends to be small.

Figs 5 and 6 show that V_H has positive values at all magnetic fields and temperatures. This indicates that the majority of carriers are holes. The Hall voltage of K–$FeCl_3$ TGICs is linear with the magnetic field. This behaviour is different from that of HOPG. The linearity of the Hall voltage with B was found for many GICs. For example, Lang [25] obtained such behaviour for AsF_5 BGIC.

The carrier concentrations, N_H, assuming a simple one-carrier model, were calculated for HOPG, Stages 2 and 5 K–$FeCl_3$ TGICs from the slope of the Hall voltage data using the equation

$$V_H = \frac{I}{N_H e t} B \tag{7}$$

where I is the current passing along the sample, e is the charge of the carriers and t is the thickness of the sample. The values of N_H at temperatures 300, 77 and 12 K are listed in Table III.

TABLE III Charge carrier concentration, N_H, for HOPG, Stages 2 and 5 K–$FeCl_3$ TGICs at temperatures 300, 77 and 12 K

Temperature (K)	HOPG ($\times 10^{26}$)	Stage 2 ($\times 10^{25}$)	Stage 5 ($\times 10^{25}$)
300	1.80	8.0	15.0
77	1.10	5.3	8.1
12	0.12	3.1	4.4

Comparing the carrier concentrations, N_H, with that calculated from the magnetoresistance measurements [26], N_{MR}, one finds some differences between the two values. This is due to the fact that the simple one-carrier model is an approximation. This might suggest that there is more than one type of charge carrier with different mobilities. This is in agreement with the results of other donor [27, 28] and acceptor BGICs [29]. In order to obtain exact values for N_{MR} and N_H, a more complicated model might be needed.

4. Conclusion

The resistivity along the c-axis for HOPG as well as Stages 2 and 5 K–$FeCl_3$ TGICs was analysed in terms of a variable range hopping conduction in parallel

with band conduction and a satisfactory fitting was obtained. The in-plane resistivity of K–$FeCl_3$ TGICs was fitted using a second-order polynomial in temperature. This indicates that at the high-temperature region, the electron–phonon scattering mechanism is dominant, while at the lower temperature region, the carrier–carrier scattering mechanism dominates. The Hall voltage, measured in a low magnetic field, indicates that holes are the dominant carriers causing the conduction. The carrier concentration was calculated from the Hall voltage at 300, 77 and 12 K.

References

1. M. S. DRESSELHAUS and G. DRESSELHAUS, *Adv. Phys.* **30** (1981) 139.
2. S. A. SOLIN, *Adv. Chem. Phys.* **49** (1982) 455.
3. B. R. YORK, S. K. HARK and S. A. SOLIN, *Phys. Rev. Lett.* **50** (1983) 1470.
4. VON K. STEINWEDE and E. STUMPP, *Z. Anorg. Allg. Chem.* **469** (1980) 101.
5. M. SUZUKI, I.OGURO and Y. JINZAKI, *J. Phys. C* **17** (1984) L575.
6. R. NIESS and E. STUMPP, *Carbon* **16** (1978) 265.
7. M. SUZUKI, P. C. CHOW and H. ZABEL, *Phys. Rev. B* **32** (1985) 6800.
8. P. LAGRANGE, A. B. RERHRHAYE, J. F. MARÊCHÉ and E. MCRAE, *Synth. Met.* **12** (1985) 201.
9. P. PERNOT, J. F. MARÊCHÉ, E. MCRAE, R. VANGÉLISTI, M. K. ALAOUI, L. PIRAUX, V. BAYOT and J.-P. ISSI, *ibid.* **34** (1989) 473.
10. D. GUÉRARD, L. ELANSARI, N. E. ELALEM, J. F. MARÊCHÉ and E. MCRAE, *ibid.* **34** (1989) 27.
11. G. O. ZIMMERMAN and A. K. IBRAHIM, US Pat. 4837377 (1989).
12. G. H. KINCHIN, *Proc. R. Soc.* **A217** (1953) 9.
13. D. E. SOULE, *Phys. Rev.* **112** (1958) 698.
14. K. T. KAWAMURA, T. SAITO and T. TSUZUKU, *J. Phys. Soc. Jpn.* **42** (1977) 574.
15. J. F. MARÊCHÉ, E. MCRAE, A. BENDRISS-RERHRHAYE and A. LAGRANGE, *J. Phys. Chem. Soc.* **47** (1986) 477.
16. E. MCRAE, J. F. MARÊCHÉ, A. B. RERHRHAYE, P. LAGRANGE and M. LELAURAIN, *Ann. Phys.* **11** (1986) 13.
17. C. A. KLEIN, *Rev. Mod. Phys.* **34** (1962) 56.
18. W. W. TYLER and A. C. WILSON, *Phys. Rev.* **89** (1953) 870.
19. J. J. MURRAY and A. R. UBBELOHDE, *Proc. R. Soc.* **A312** (1969) 371.
20. R. POWERS, A. K. IBRAHIM, G. O. ZIMMERMAN and M. TAHAR, *Phys. Rev.* **B38** (1988) 680.
21. B. I. SHKLOVSKII and A. L. EFROS, in "Electronic Properties of Doped Semiconductors" (Springer, Berlin, 1984).
22. K. SUGIHARA, I. SHIOZAKI, S. M. SAMPERE, M. SUZUKI, J. T. NICHOLIS and G. DRESSELHAUS, *Synth. Met.* **34** (1989) 543.
23. I. L. SPAIN, A. R. UBBELOHDE and D. A. YOUNG, *Phil. Trans. R. Soc.* **A262** (1967) 345.
24. T. TSUZUKU and T. TAKEZAWA, *Philos. Mag.* **25** (1972) 929.
25. W. LANG, *Synth. Met.* **34** (1989) 491.
26. O. EL-SHAZLY, S. G. TAWFIK A. K. IBRAHIM, I. H. IBRAHIM, and E. F. El-WAHIDY, *J. Phys. D.* (1993) accepted for publication.
27. D. GUÈRARD, G. M. T. FOLY, M. ZANINI and J. E. FISCHER, *Nuovo Cimento* **B38** (1977) 410.
28. H. SUEMATSU, K. HIGUCHI and S. TANUMA, *J. Phys. Soc. Jpn.* **48** (1980) 1541.
29. O. EL-SHAZLY and A. I. ABOU-ALI, *J. Phys. Chem. Solids* **52** (1991) 643.

Received 28 July 1992
and accepted 3 February 1993